Classical Forcefield Model

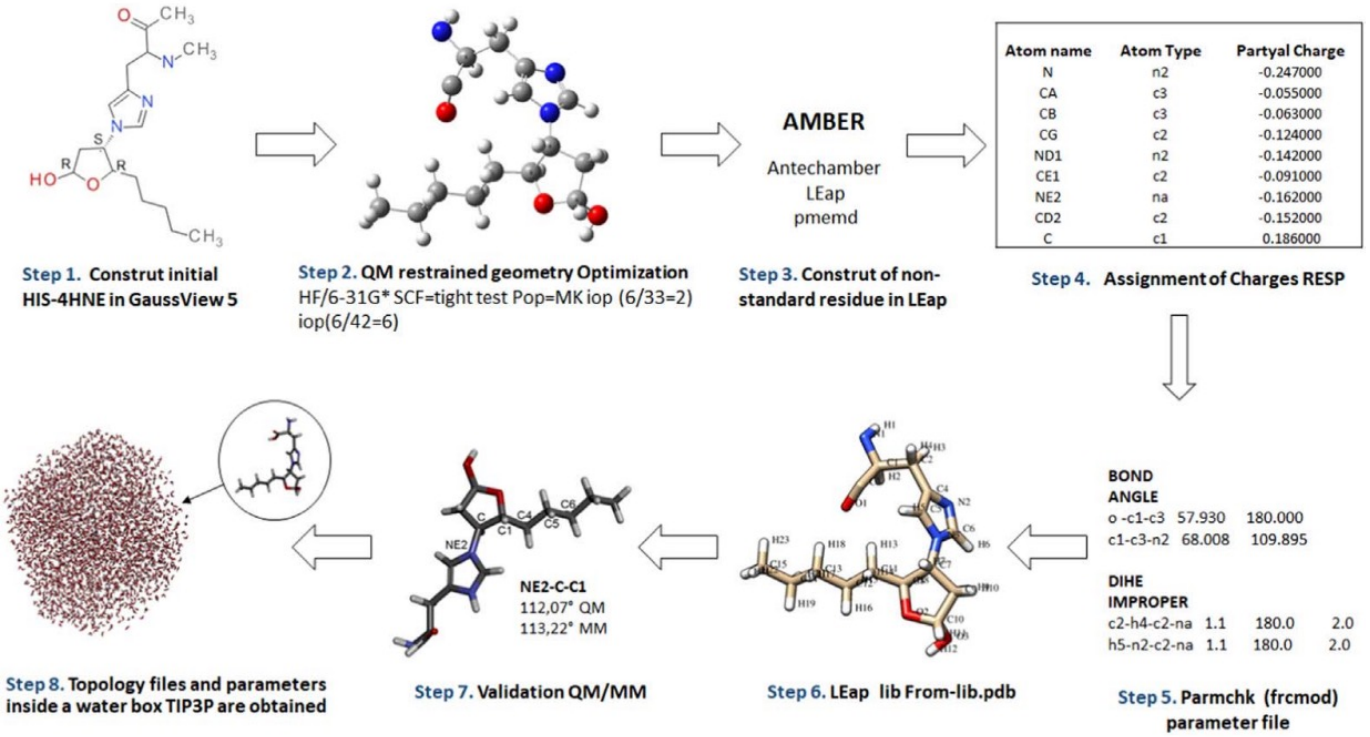

2024 Winter Son Lab Seminar

January 12th, 2024

SeungBin Hong

Data in Brief., ***2018***, *21, 2581-2589*

Content

History of Forcefield

Physically incorrect results, several artifacts and Breakthrough

Multiple perspectives

History of Forcefield

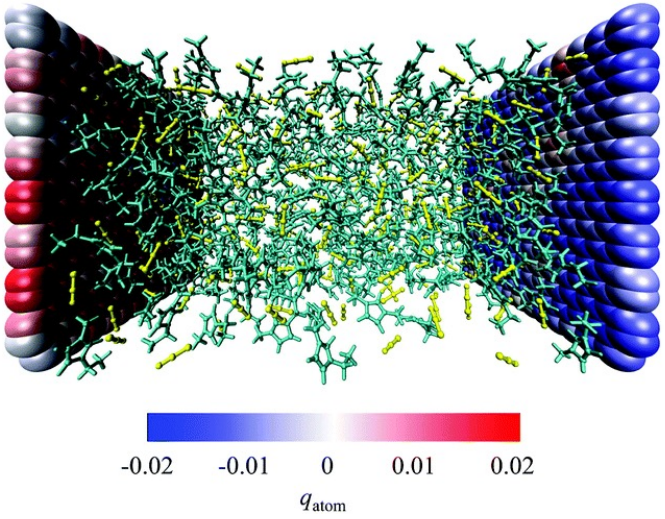

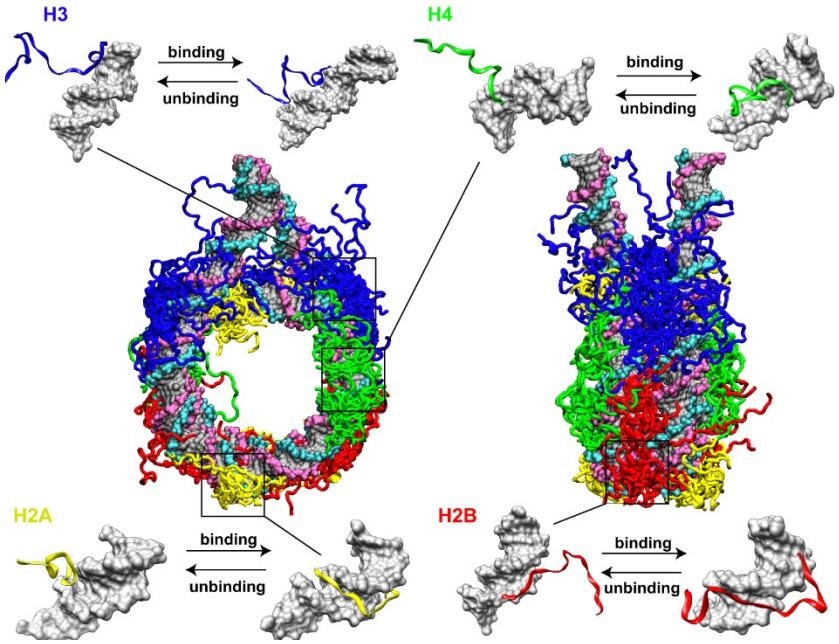

Phys. Chem. Chem. Phys., ***2019***, *21, 6790-6800*
Nat Commun, 2021, 12, 5280

History of Forcefield

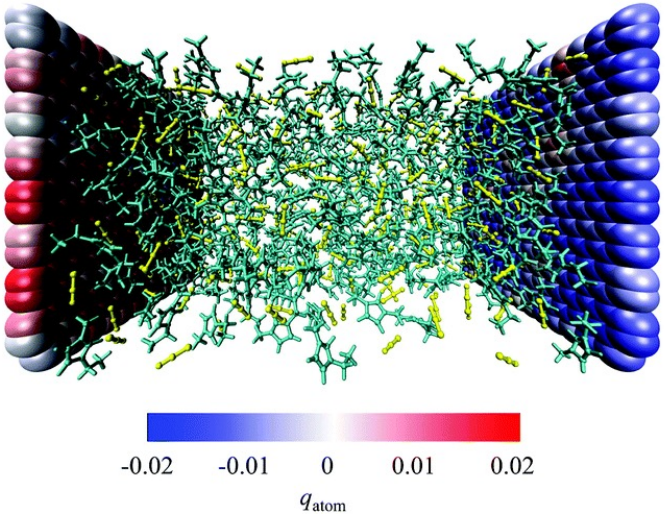

$$\boldsymbol{F = ma}$$

$$\boldsymbol{F = -\frac{\partial\big(U(x)\big)}{\partial(x)}}$$

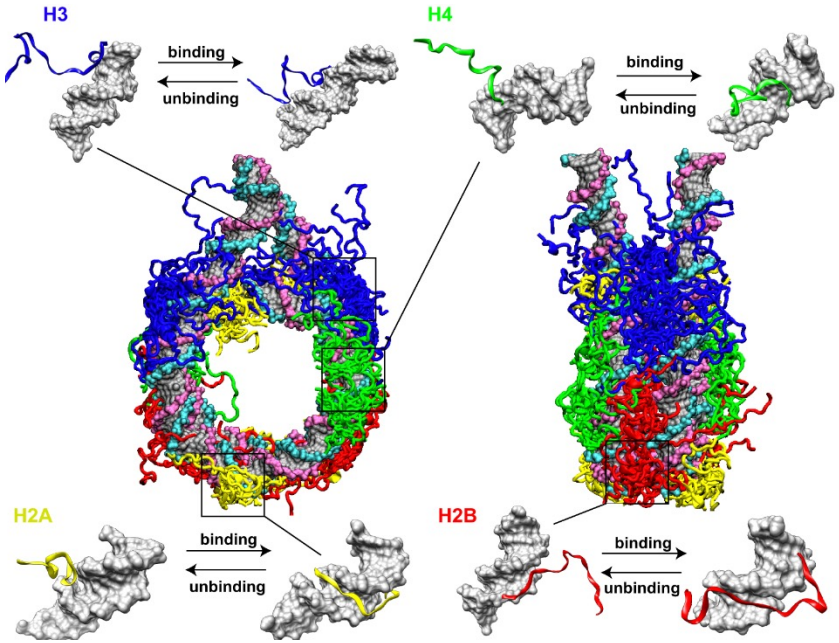

Molecular dynamics of Monte Carlo Simulations usually adopt 'Force Field'

Phys. Chem. Chem. Phys., ***2019***, *21, 6790-6800*
Nat Commun, 2021, 12, 5280

History of Forcefield

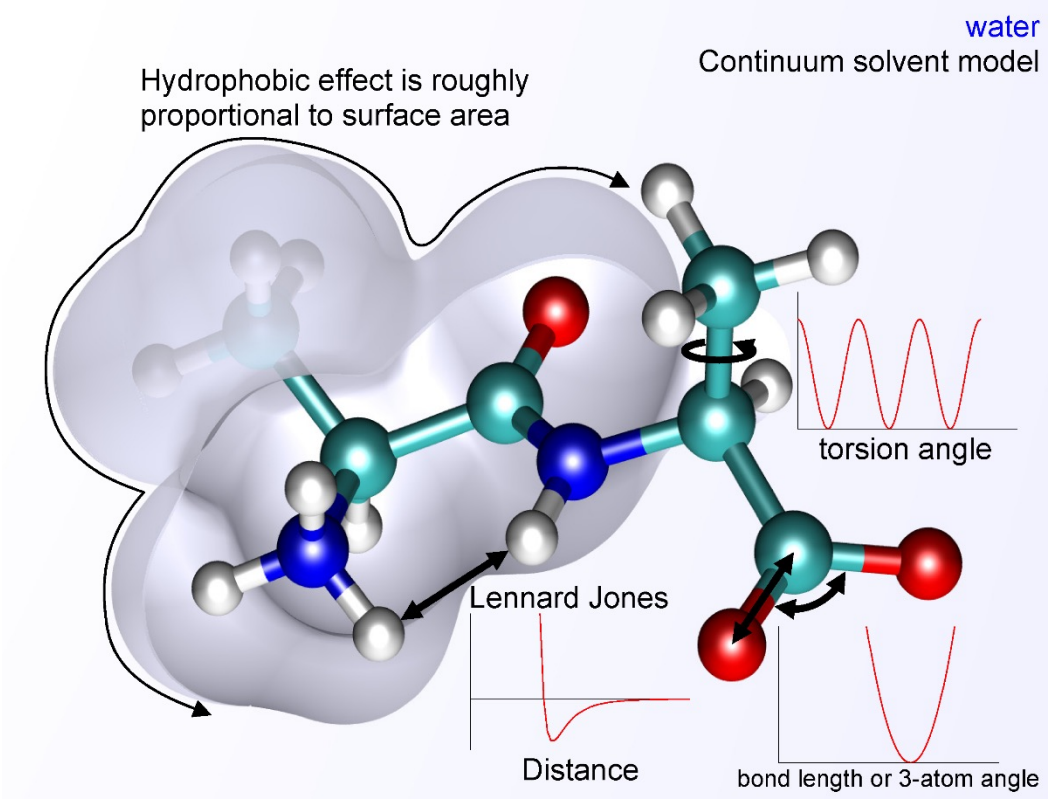

Tetrahedron, Rev , ***2021***, *79*

History of Forcefield

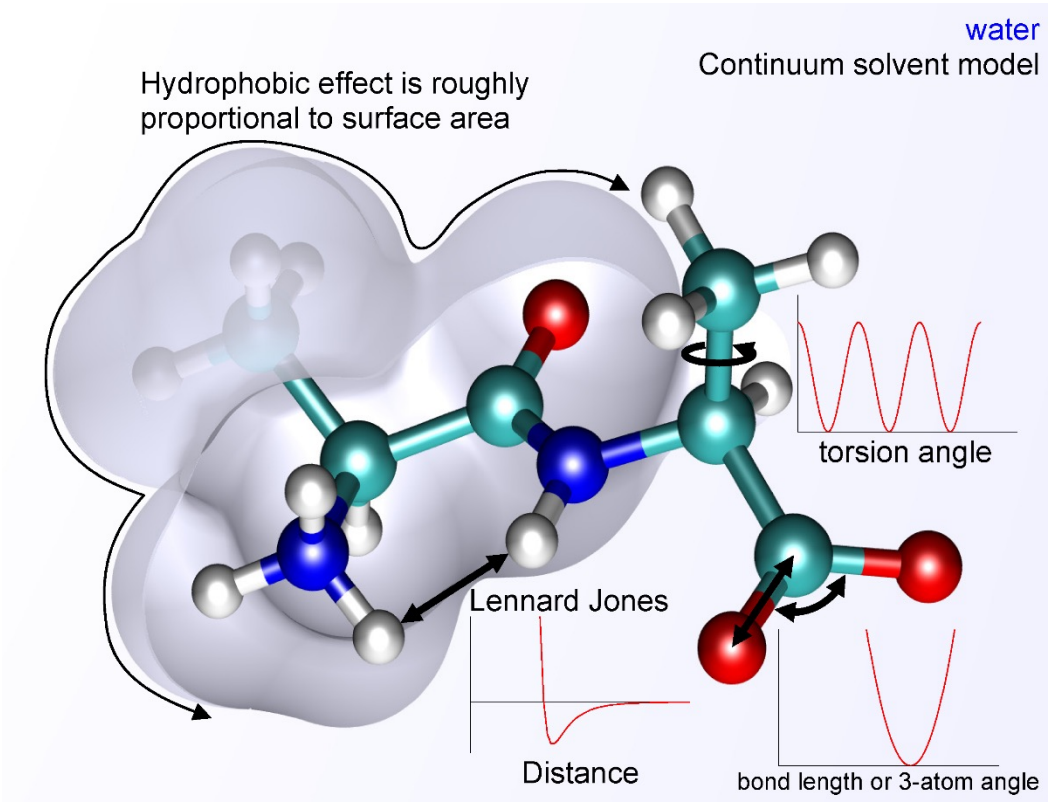

$$V(R_1, R_2, \ldots) = \sum_i \frac{K_i^r}{2}\left(r_i - r_{0,1}\right)^2 + \sum_j \frac{K_j^\theta}{2}\left(\theta_i - \theta_{0,j}\right)^2 + \sum_l \frac{K_l^\psi}{2}\left[1 - cos\left(m(\psi_i - \psi_{0,l})\right)\right]$$
$$+ \sum_{n\le m}^{N_{at}} \epsilon_{n,m}\left[\left(\frac{\sigma_{n,m}}{|R_n - R_m|}\right)^{12} - \left(\frac{\sigma_{n,m}}{|R_n - R_m|}\right)^{6}\right] + \sum_{n\le m}^{N_{at}} \frac{1}{4\pi\epsilon_0}\frac{q_n q_m}{|R_n - R_m|}$$

Tetrahedron, Rev , ***2021***, *79*

History of Forcefield

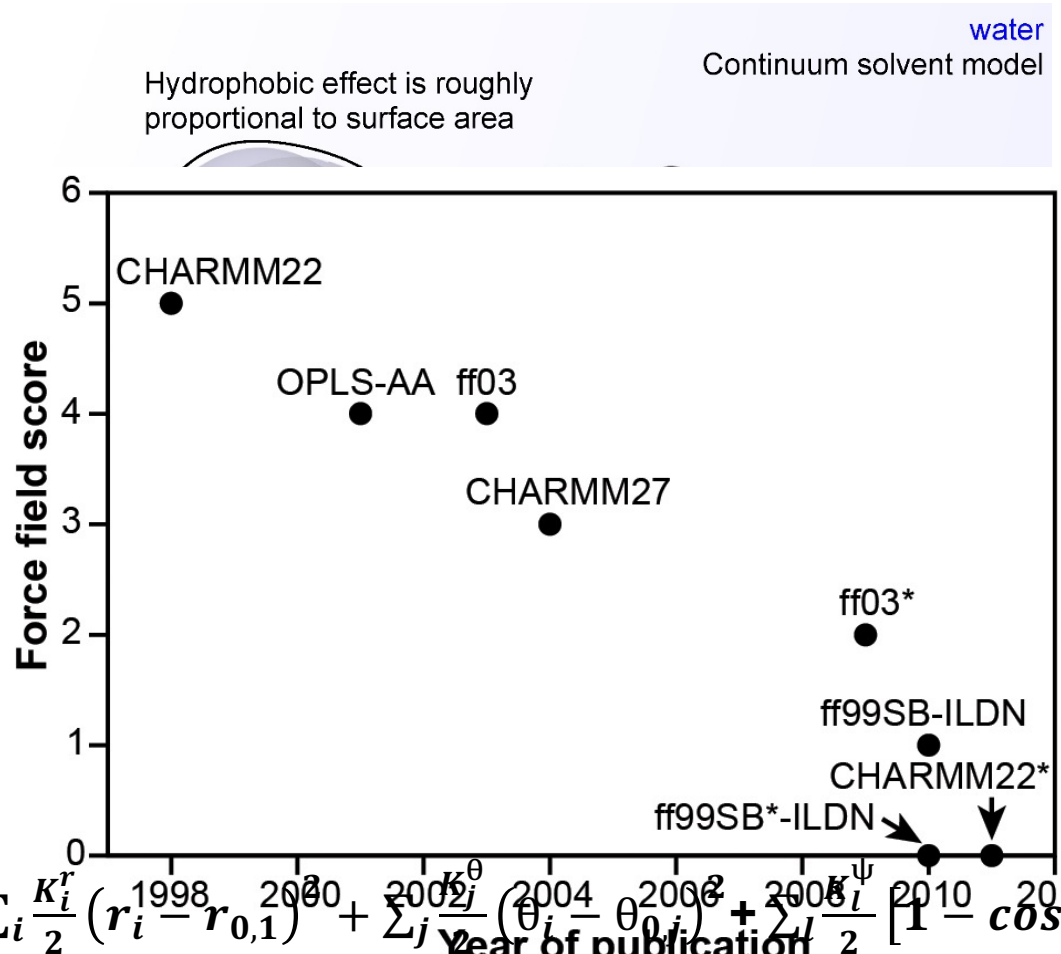

$$V(R_1, R_2, \ldots) = \sum_i \frac{K_i^r}{2}\left(r_i - r_{0,1}\right)^2 + \sum_j \frac{K_j^\theta}{2}\left(\theta_i - \theta_{0,j}\right)^2 + \sum_l \frac{K_l^\psi}{2}\left[1 - \cos\left(m(\psi_i - \psi_{0,l})\right)\right]$$
$$+ \sum_{n \le m}^{N_{at}} \epsilon_{n,m}\left[\left(\frac{\sigma_{n,m}}{|R_n - R_m|}\right)^{12} - \left(\frac{\sigma_{n,m}}{|R_n - R_m|}\right)^{6}\right] + \sum_{n \le m}^{N_{at}} \frac{1}{4\pi\epsilon_0}\frac{q_n q_m}{|R_n - R_m|}$$

Tetrahedron, Rev , ***2021***, 79

PLOS ONE, ***2012***, 7, e32131

History of Forcefield

Quadratic Energy function ➔ $\sum_i \frac{K_i^r}{2}\left(r_i - r_{0,1}\right)^2$ ***or*** $\sum_j \frac{K_j^\theta}{2}\left(\theta_i - \theta_{0,j}\right)^2$

NB Pairwise interaction ➔ $\sum_{n\leq m}^{N_{at}} \epsilon_{n,m}\left[\left(\frac{\sigma_{n,m}}{|R_n - R_m|}\right)^{12} - \left(\frac{\sigma_{n,m}}{|R_n - R_m|}\right)^{6}\right] + \sum_{n\leq m}^{N_{at}} \frac{1}{4\pi\epsilon_0}\frac{q_n q_m}{|R_n - R_m|}$

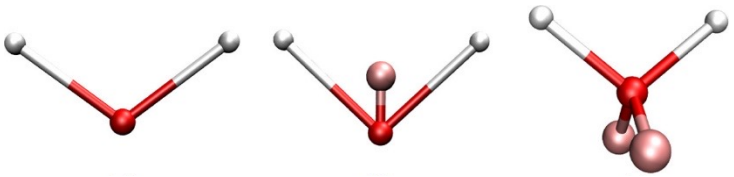

	SPCE	TIP4P	TIP5P
q(O or L)	-0.8476	-1.04	-0.241
q(H)	0.4238	0.52	0.241

ACS Omega, 2020, 5, 39, 25087-25094
https://en.wikipedia.org/wiki/Water_model

History of Forcefield

Quadratic Energy function ➔ $\sum_i \frac{K_i^r}{2}\left(r_i - r_{0,1}\right)^2$ ***or*** $\sum_j \frac{K_j^\theta}{2}\left(\theta_i - \theta_{0,j}\right)^2$

$D_e\left(1 - e^{(-a(r-r_e))}\right)^2$ **?**

NB Pairwise interaction ➔ $\sum_{n\leq m}^{N_{at}} \epsilon_{n,m}\left[\left(\frac{\sigma_{n,m}}{|R_n - R_m|}\right)^{12} - \left(\frac{\sigma_{n,m}}{|R_n - R_m|}\right)^{6}\right] + \sum_{n\leq m}^{N_{at}} \frac{1}{4\pi\epsilon_0}\frac{q_n q_m}{|R_n - R_m|}$

$\left[Aexp(-B|R_n - R_m|) - \left(\frac{\sigma_{n,m}}{|R_n - R_m|}\right)^6\right]$

$\sigma_{ij} = \sqrt{\sigma_i \sigma_j}$ **or** $\sigma_{ij} = \frac{\sigma_i + \sigma_j}{2}$ **etc…**

$\varepsilon_{ij} = \sqrt{\varepsilon_i \varepsilon_j}$ $\varepsilon_{ij} = \sqrt{\varepsilon_i \varepsilon_j}$

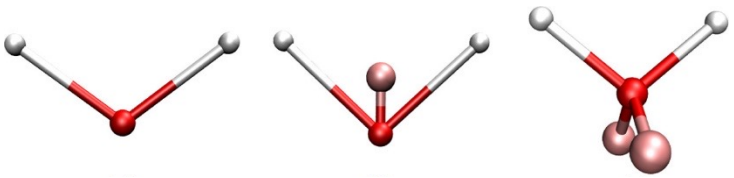

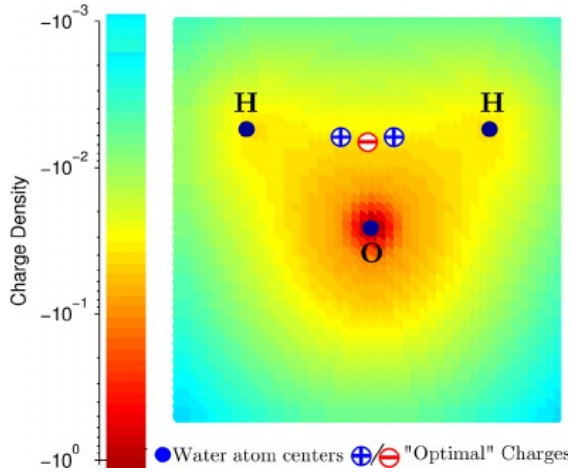

ACS Omega, 2020, 5, 39, 25087-25094
J. Phys. Chem. Lett., ***2014****, 5, 3863-3871.*

Physically incorrect results, several artifacts and Breakthrough

Case I . The monovalent ions' inaccuracies with AMBER-99 Forcefield

With AMBER-99 Forcefield's, too strong interaction between 1 : 1 electrolytes cause unphysical clusters.

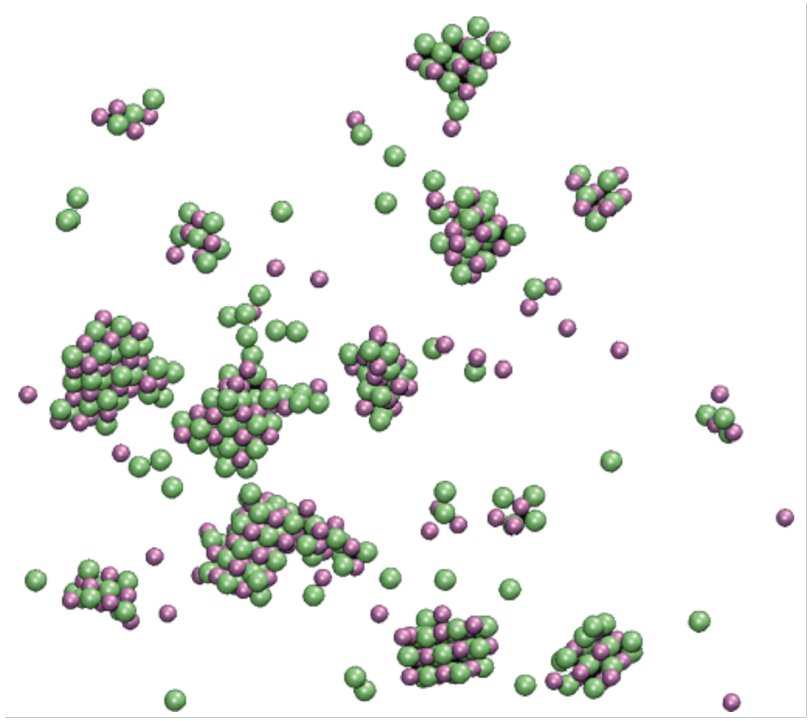

salt	AMBER-99	OPLS	conductometric measurement
NaCl	0.96 ± 0.14	0.76 ± 0.05	0.82
KCl	13 ± 1.9	0.57 ± 0.04	0.53
CsCl	19 ± 2.9	0.49 ± 0.07	0.62

salt	molten liquid (Å)	crystal lattice (Å)	preferred contact distances obtained from analysis of simulated RDFs	
			AMBER-99 (Å)	OPLS (Å)
NaCl	2.72−2.78	2.76−2.83	**2.74**	2.74
KCl	3.06	3.14−3.19	**3.00**	3.10
CsCl	3.38−3.40	3.48−3.50	**3.25**	3.48

J. Phys. Chem. B., ***2007***, 111, 41, 11884-11887.

Physically incorrect results, several artifacts and Breakthrough

Case I . The monovalent ions' inaccuracies with AMBER-99 Forcefield

atom (AMBER-99)	σ (Å)	ϵ (kJ/mol)	atom (OPLS)	σ (Å)	ϵ (kJ/mol)
Na^+	3.32840	1.15897×10^{-2}	Na^+	3.33045	1.15980×10^{-2}
K^+	4.72302	1.37235×10^{-3}	K^+	4.93463	1.37235×10^{-3}
Cs^+	6.04920	3.3723×10^{-4}	Cs^+	6.71600	3.38904×10^{-4}
Cl^-	4.40104	4.184×10^{-1}	Cl^-	4.41724	4.92833×10^{-1}
O (TIP3P)	3.15061	6.36396×10^{-1}	O (TIP3P)	3.15061	6.36396×10^{-1}
O2 (DMP^-)	2.95992	8.7864×10^{-1}	O2	2.96000	8.7864×10^{-1}
OS (DMP^-)	3.00001	7.11280×10^{-1}	OS	3.00000	7.11280×10^{-1}

[a] Åqvist's cation parameters as specified by the AMBER-99[7] and OPLS[9] forcefields. The parameters for the TIP3P water model are taken from Jorgensen et al.[31] Note that AMBER adopts the Cl^- of Smith and Dang[20] while OPLS adopts the Cl^- of Chandresekhar et al.[21] The last two rows show the AMBER-99 L-J parameters for the phosphate oxygen atoms of the DMP^- anion.

Nucleic acids' Polyphosphate backbone

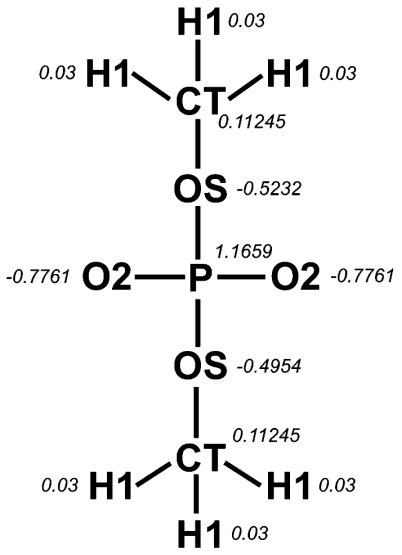

J. Phys. Chem. B., ***2007***, 111, 41, 11884-11887.

Physically incorrect results, several artifacts and Breakthrough

Case I . The monovalent ions' inaccuracies with AMBER-99 Forcefield

atom (AMBER-99)	σ (Å)	ϵ (kJ/mol)	atom (OPLS)	σ (Å)	ϵ (kJ/mol)
Na^+	3.32840	1.15897×10^{-2}	Na^+	3.33045	1.15980×10^{-2}
K^+	4.72302	1.37235×10^{-3}	K^+	4.93463	1.37235×10^{-3}
Cs^+	6.04920	3.3723×10^{-4}	Cs^+	6.71600	3.38904×10^{-4}
Cl^-	4.40104	4.184×10^{-1}	Cl^-	4.41724	4.92833×10^{-1}
O (TIP3P)	3.15061	6.36396×10^{-1}	O (TIP3P)	3.15061	6.36396×10^{-1}
O2 (DMP^-)	2.95992	8.7864×10^{-1}	O2	2.96000	8.7864×10^{-1}
OS (DMP^-)	3.00001	7.11280×10^{-1}	OS	3.00000	7.11280×10^{-1}

[a] Åqvist's cation parameters as specified by the AMBER-99[7] and OPLS[9] forcefields. The parameters for the TIP3P water model are taken from Jorgensen et al.[31] Note that AMBER adopts the Cl^- of Smith and Dang[20] while OPLS adopts the Cl^- of Chandresekhar et al.[21] The last two rows show the AMBER-99 L-J parameters for the phosphate oxygen atoms of the DMP^- anion.

Nucleic acids' Polyphosphate backbone

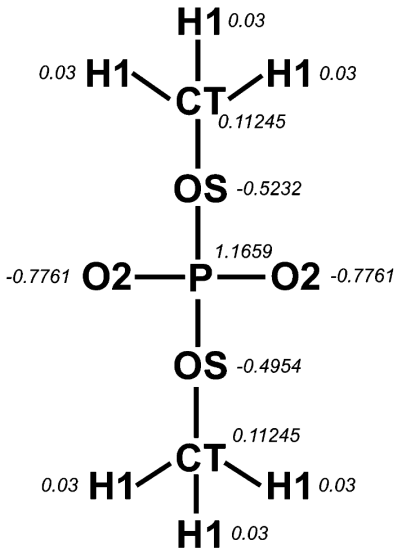

ion	simulated cation−DMP^- oxygen distance (Å)[b]	crystallographic cation−DMP^- oxygen distance (Å)[23]
Na^+	2.35 ± 0.10	2.21/2.41
K^+	2.70 ± 0.15	2.43/2.80

Matching well

J. Phys. Chem. B., ***2007***, 111, 41, 11884-11887.

Case II . Kirkwood-Buff Forcefield

Biomolecular FFs encountered include:

1) an incorrect balance between α and β secondary structures usually related to the ϕ/ψ rotational potential surfaces ; simulated melting temperatures of small peptides (when observed to be stable) were often significantly larger than experimental

2) inability to accurately rank ligands in docking calculations even when the predicted ligand pose was correct.

Physically incorrect results, several artifacts and Breakthrough

Case II . Kirkwood-Buff Forcefield

Biomolecular FFs encountered include:

1) an incorrect balance between α and β secondary structures usually related to the ϕ/ψ rotational potential surfaces ; simulated melting temperatures of small peptides (when observed to be stable) were often significantly larger than experimental

2) inability to accurately rank ligands in docking calculations even when the predicted ligand pose was correct.

The KB theory is an exact theory of solution mixtures that relates integrals over the various underlying molecular distributions to the observed thermodynamic behavior of the solution.

The KB theory provides a link between the microscopic "structure" of a solution and the corresponding thermodynamic properties of that solution.

$$G_{\alpha\beta} = G_{\beta\alpha} \equiv 4\boldsymbol{\pi} \int_0^\infty \left[g_{\alpha\beta}(r) - 1\right] r^2 dr$$

$$g_{\alpha\beta}(r) = e^{-\beta W_{\alpha\beta}(r)}$$

J. Chem. Theory Comput. ***2021****, 17, 5, 2964–2990*

Physically incorrect results, several artifacts and Breakthrough

Case II . Kirkwood-Buff Forcefield

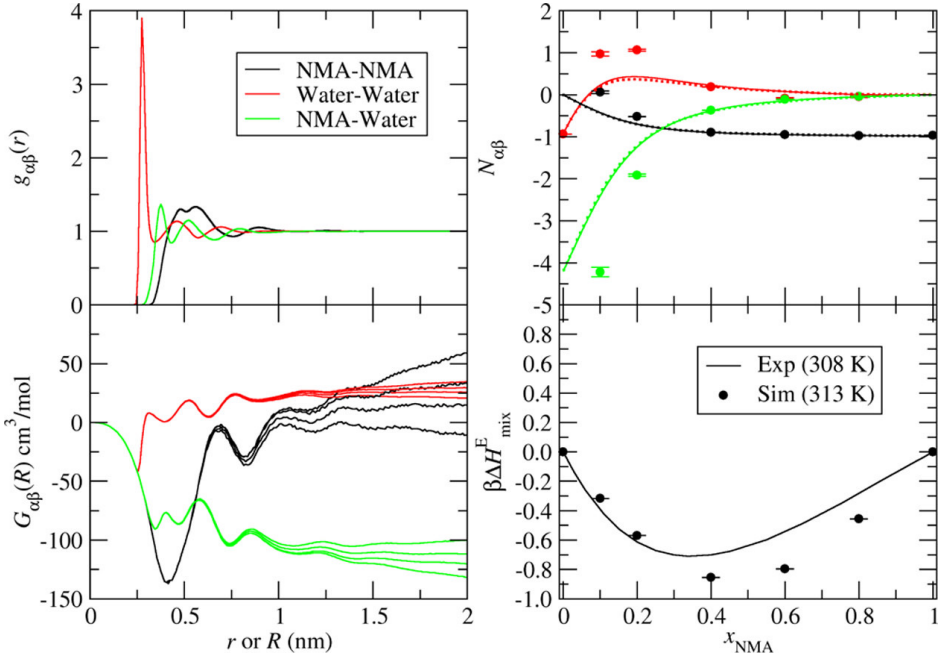

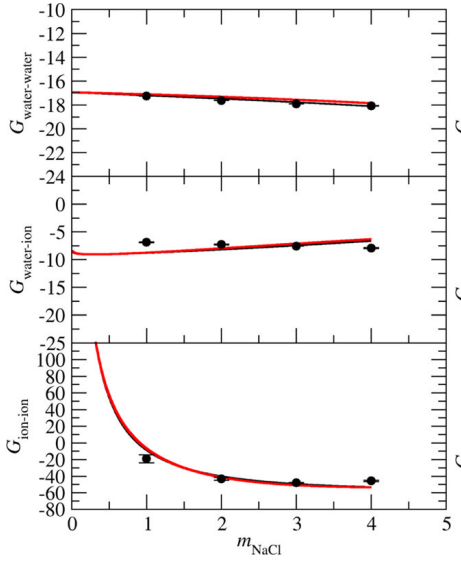

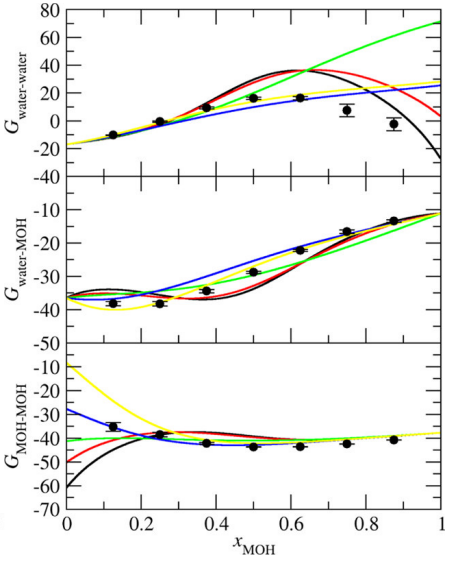

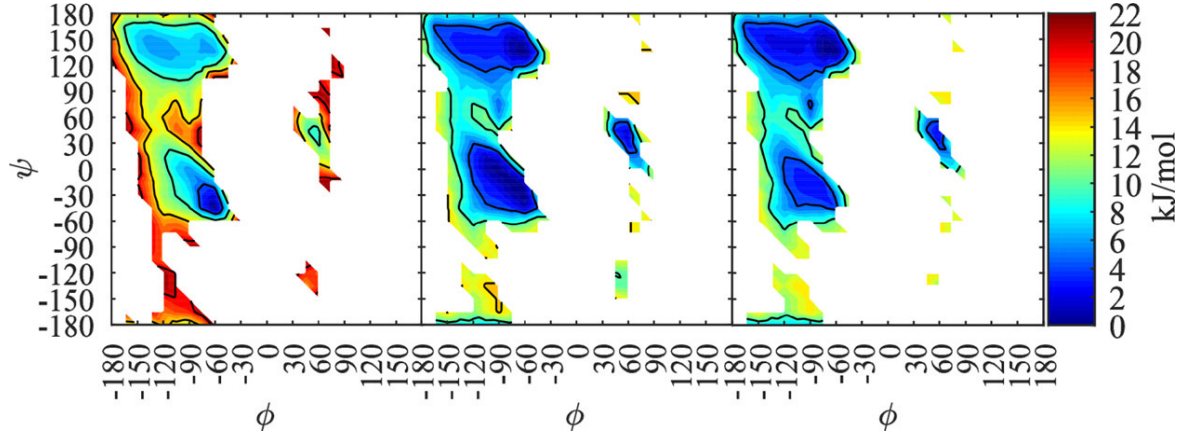

J. Chem. Theory Comput. ***2021***, *17, 5, 2964–2990*

Physically incorrect results, several artifacts and Breakthrough

Case III . Champaign-Urbana NBFIX correction

MD characterization of denatured conformations remains challenging in part because of the inaccuracies of the molecular forcefields that have been calibrated to reproduce the properties of folded biomolecules.

Largely, the MD community is in agreement that the approximate description of molecular interactions **employed by the fixed-charge models strengthens attractive solute–solute interactions**, which causes artificial aggregation of denatured proteins ormultimeric assemblies.

Physically incorrect results, several artifacts and Breakthrough

Case III . Champaign-Urbana NBFIX correction

MD characterization of denatured conformations remains challenging in part because of the inaccuracies of the molecular forcefields that have been calibrated to reproduce the properties of folded biomolecules.

Largely, the MD community is in agreement that the approximate description of molecular interactions **employed by the fixed-charge models strengthens attractive solute–solute interactions**, which causes artificial aggregation of denatured proteins ormultimeric assemblies.

One way to dealing this problem, we discuss an alternative approach for improving the MD force fields that **surgically corrects pair-specific Lennard-Jones(LJ) parameters without modifying solute–water interactions**.

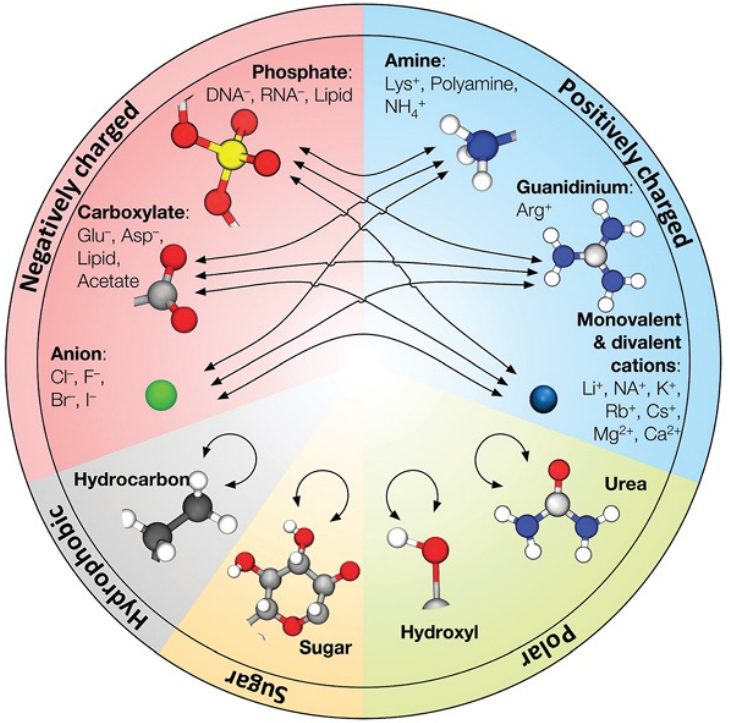

J. Chem. Theory Comput. ***2021***, *17, 5, 2964–2990*

Physically incorrect results, several artifacts and Breakthrough

Case III . Champaign-Urbana NBFIX correction

The osmotic pressure of a solution can be related to its concentration by introducing a concentration-dependent factor, the osmotic coefficient ϕ(c), p(c)=**ϕ(c)**cRT.

Broadly speaking, ϕ values smaller than 1 indicate attractive interactions between the osmolytes, which decrease the effective osmolyte concentration to ϕc as the osmolytes form complexes.

Conversely, ϕ values larger than 1 indicate repulsive interactions that effectively increase the solute concentration to ϕc.

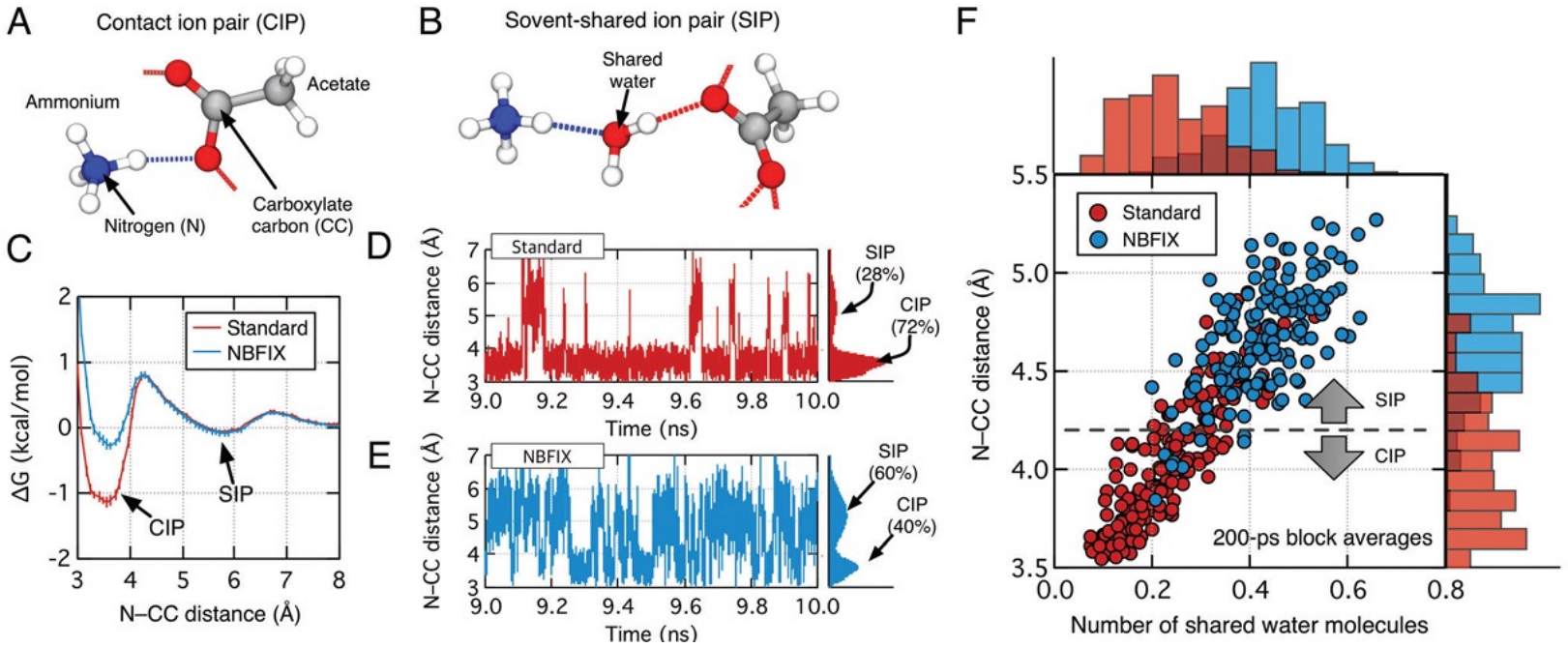

J. Chem. Theory Comput. ***2021****, 17, 5, 2964–2990*

Physically incorrect results, several artifacts and Breakthrough

Case IV . Simulating water with rigid non-polarizable models

- Properties of the gas phase
- Critical pressure
- Simultaneous matching of the vaporisation enthalpy and the critical temperature
- Simultaneous matching of the melting temperature and the maximum in density
- Heat capacity
- The third law of Thermodynamics
- Dielectric constant
- Extremely high pressure region of the phase diagram
- Chemical limits

➔ Inclusion Many Body forces (Polarization, three body forces)
➔ Inclusion of nuclear quantum effects
➔ Considering Electron Transfer

Phys. Chem. Chem. Phys., ***2011***,*13, 19663-19688*

Physically incorrect results, several artifacts and Breakthrough

Case IV . Simulating water with rigid non-polarizable models

For including an accurate representation of Born-Oppenheimer potential , adding “Many-body potential” in predefined analytical functions can be an option.

$$V_N(\mathrm{r}_1, \ldots, \mathrm{r}_N) = \sum_{i=1}^{N} V_{1\mathrm{B}}(\mathrm{r}_i) + \sum_{i<j}^{N} V_{2\mathrm{B}}(\mathrm{r}_i, \mathrm{r}_j) + \sum_{i<j<k}^{N} V_{3\mathrm{B}}(\mathrm{r}_i, \mathrm{r}_j, \mathrm{r}_k) + \ldots + V_{\mathrm{NB}}(\mathrm{r}_1, \mathrm{r}_2, \mathrm{r}_3, \ldots, \mathrm{r}_N)$$

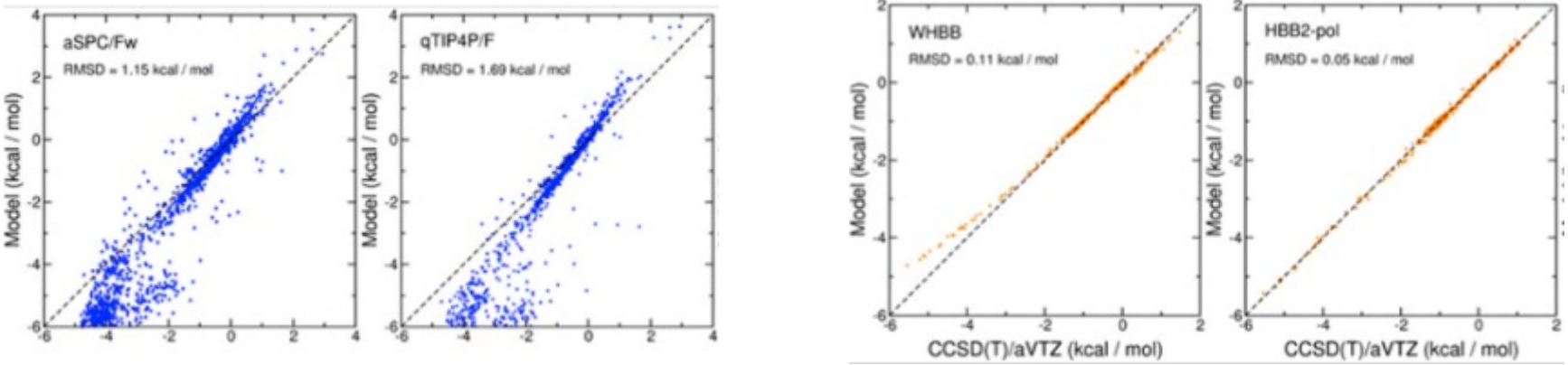

The x_{axes} are the BSSE-corrected CCSD(T) reference energies calculated with the aug-ccpVTZ (aVTZ) basis set for~1400 water dimers.

The y_{axes} are the corresponding energies calculated with the different water PEFs.

Physically incorrect results, several artifacts and Breakthrough

Case V . Too strong Non-Bonded interaction between molecules

1) The physical and chemical properties of ionic liquids are largely dependent upon solvent structure, including the organization resulting from standard ion−ion interactions and specific hydrogen bonding between cations and anions.

The general trend seen among ionic liquid forcefields is accurate densities but **dynamical properties that are too slow and vaporization enthalpies that are too large.**

J. Chem. Theory Comput. ***2017****, 13, 12, 6131−6145*
J. Chem. Theory Comput. ***2018****, 14, 12, 6690−6700*

Case V . Too strong Non-Bonded interaction between molecules

1) The physical and chemical properties of ionic liquids are largely dependent upon solvent structure, including the organization resulting from standard ion−ion interactions and specific hydrogen bonding between cations and anions.

The general trend seen among ionic liquid forcefields is accurate densities but **dynamical properties that are too slow and vaporization enthalpies that are too large.**

2) When applying carbohydrate force fields such as CHARMM, OPLS-AA, GROMOS, accharide solutions is the **overestimation of the sugar−sugar interactions**, leading to strong sugar aggregation at elevated sugar concentration.

Both thermodynamic properties (densities, activity coefficients, thermody-namic factors, second virial coefficients, etc.) and transport properties (shear viscosities, diffusion coefficients, etc.) of concentrated solutions are generally not well reproduceded.

J. Chem. Theory Comput. ***2017****, 13, 12, 6131−6145*
J. Chem. Theory Comput. ***2018****, 14, 12, 6690−6700*

Physically incorrect results, several artifacts and Breakthrough

Case V . Too strong Non-Bonded interaction between molecules

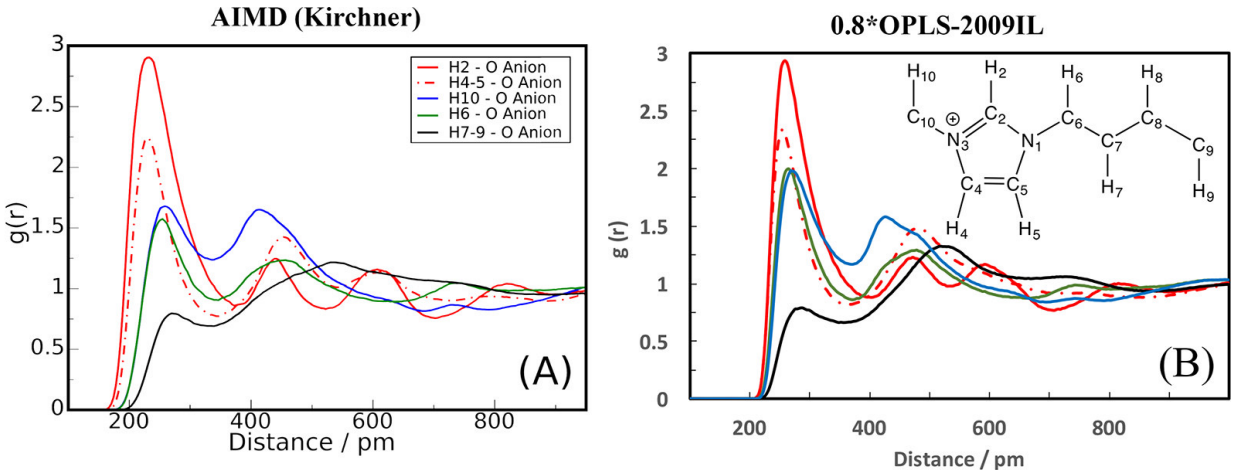

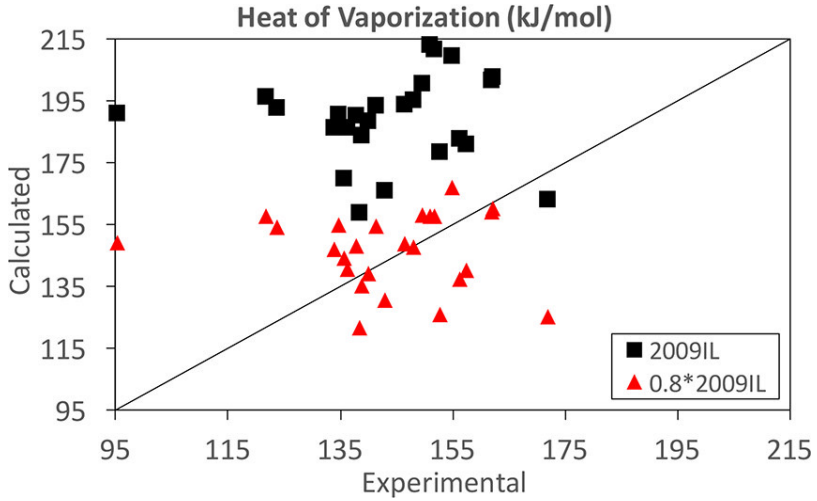

J. Chem. Theory Comput. ***2017****, 13, 12, 6131−6145*
J. Chem. Theory Comput. ***2018****, 14, 12, 6690−6700*

Physically incorrect results, several artifacts and Breakthrough

Case V . Too strong Non-Bonded interaction between molecules

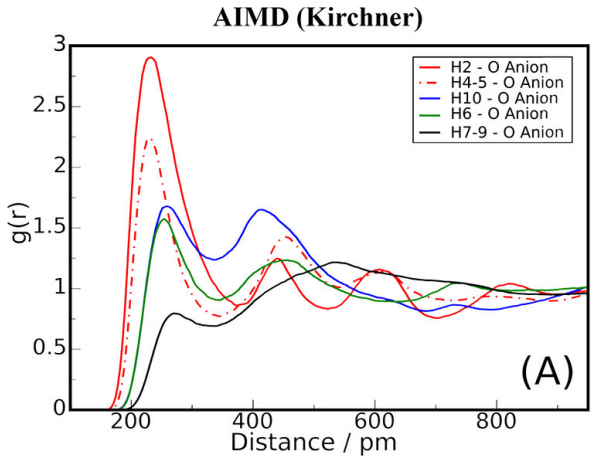

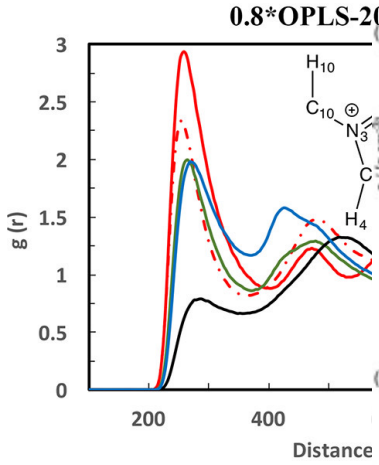

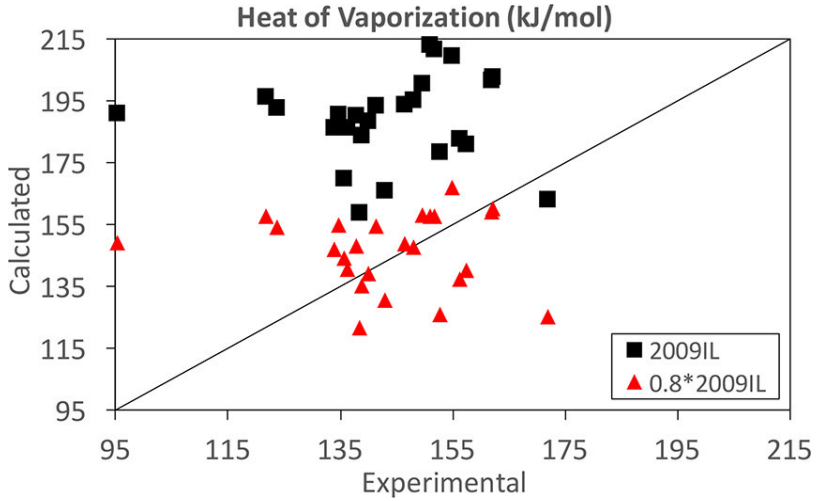

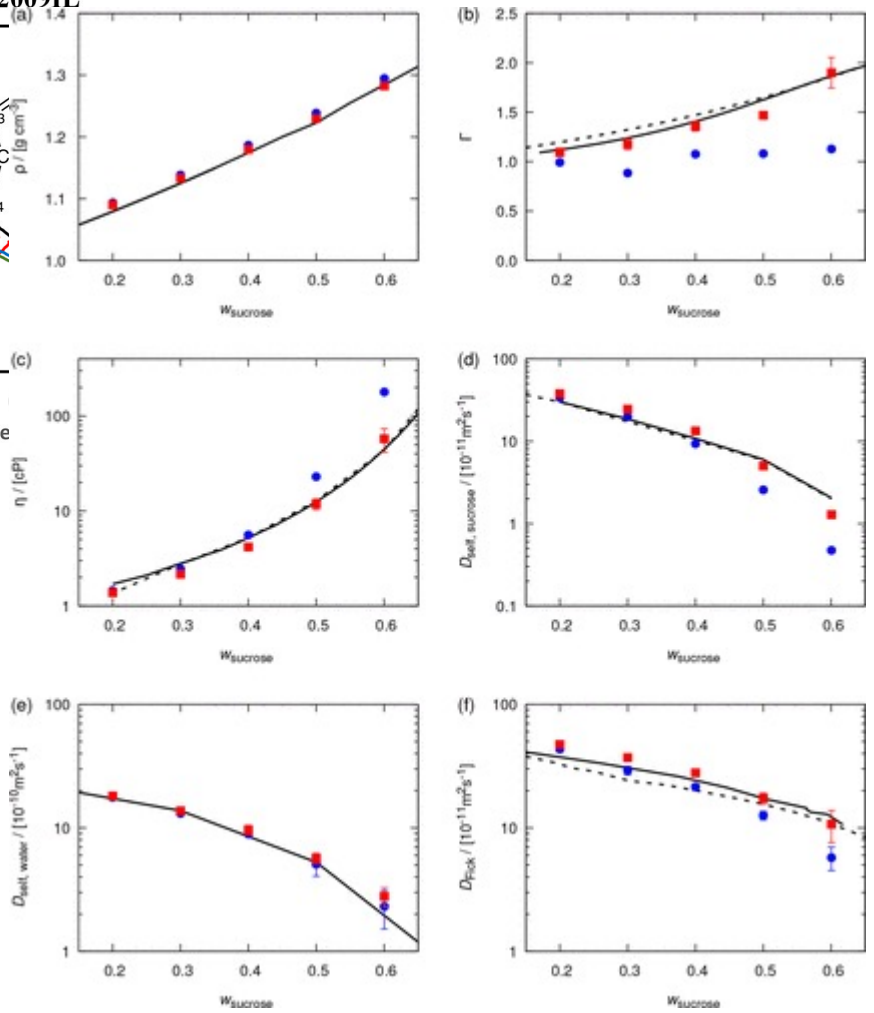

J. Chem. Theory Comput. ***2017****, 13, 12, 6131−6145*
J. Chem. Theory Comput. ***2018****, 14, 12, 6690−6700*

Multiple perspectives

Case I . Physically-Motivated Force Fields from Symmetry-Adapted Perturbation Theory

Historically, such intermolecular forcefields have been dominated **by simple functional forms dictated more by computational convenience** than by physical significance (e.g.,Lennard-Jones) and empirically parametrized on the basis of prior experimental data.

To get more accurate and “physically-motivated” (exchange, electrostatic , induction and dipersion) ab initio force fields, new force field framework based on symmetry-adapted perturbation theory (SAPT).

*J. Phys. Chem. A **2013**, 117, 10, 2053–2066*

Multiple perspectives

Case I . Physically-Motivated Force Fields from Symmetry-Adapted Perturbation Theory

Historically, such intermolecular forcefields have been dominated **by simple functional forms dictated more by computational convenience** than by physical significance (e.g.,Lennard-Jones) and empirically parametrized on the basis of prior experimental data.

To get more accurate and "physically-motivated" (exchange, electrostatic , induction and dipersion) ab initio force fields, new force field framework based on symmetry-adapted perturbation theory (SAPT).

$$E_{int} = E_{elec} + E_{exch} + E_{pol} + E_{disp} + E_{\delta hf}$$

$$E_{elec} = E_{pol}^{(1)}$$

$$E_{exch} = E_{exch}^{(1)}$$

$$E_{pol} = E_{ind}^{(2)} + E_{ind-exch}^{(2)}$$

$$E_{elec} = E_{disp}^{(2)} + E_{disp-exch}^{(2)}$$

$$E_{\text{elec}} \cong \sum_{i,j} f_1(B_{ij}, r_{ij}) \frac{q_i q_j}{r_{ij}} + \sum_{i,j} A_{ij}^{\text{elec}} \exp(-B_{ij} r_{ij})$$

$$E_{\text{exch}} \cong \sum_{i,j} A_{ij}^{\text{exch}} \exp(-B_{ij} r_{ij})$$

$$E_{\text{pol}} \cong U_{\text{shell}}^{(2)} + \sum_{i,j} A_{ij}^{\text{ind}} \exp(-B_{ij} r_{ij})$$

$$E_{\text{disp}} \cong - \sum_{n=6,8,10,12} \sum_{i,j} f_n(B_{ij}, r_{ij}) \frac{C_n^{ij}}{r_{ij}^n}$$

$$E_{\delta\text{hf}} \cong U_{\text{shell}}^{\Delta\text{SCF}} + \sum A_{ij}^{\delta\text{hf}} \exp(-B_{ij} r_{ij})$$

$$U_{\text{tot}} = \sum_{i,j} f_1(B_{ij}, r_{ij}) \frac{q_i q_j}{r_{ij}} + \sum_{i,j} \left(A_{ij}^{\text{tot}} \exp(-B_{ij} r_{ij}) - \sum_{n=6,8,10,12} f_n(B_{ij}, r_{ij}) \frac{C_n^{ij}}{r_{ij}^n} \right) + U_{\text{shell}}$$

$$B_2 = 2\pi \int (1 - \langle \exp[-\beta U_{\text{inter}}(\xi)] \rangle_{\alpha_1 \alpha_2}) \xi^2 \, d\xi$$

J. Phys. Chem. A ***2013****, 117, 10, 2053–2066*

Multiple perspectives

Case I . Physically-Motivated Force Fields from Symmetry-Adapted Perturbation Theory

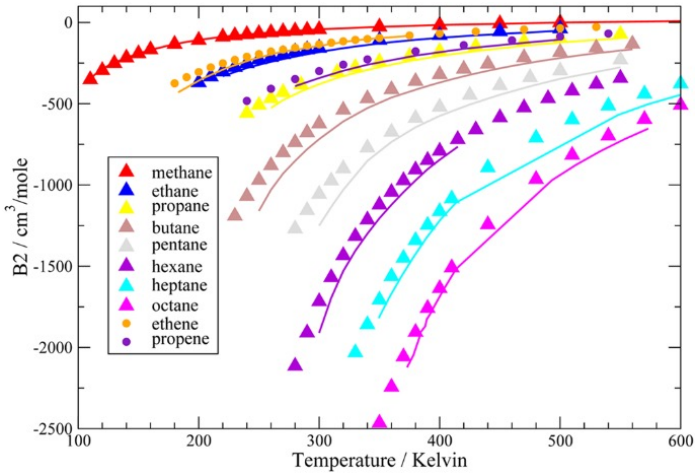

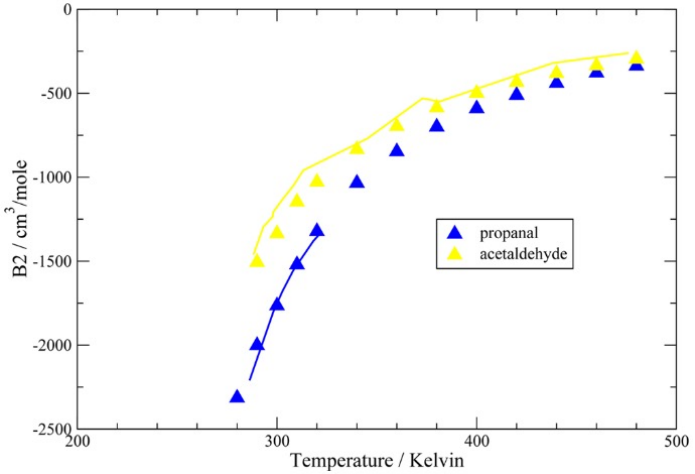

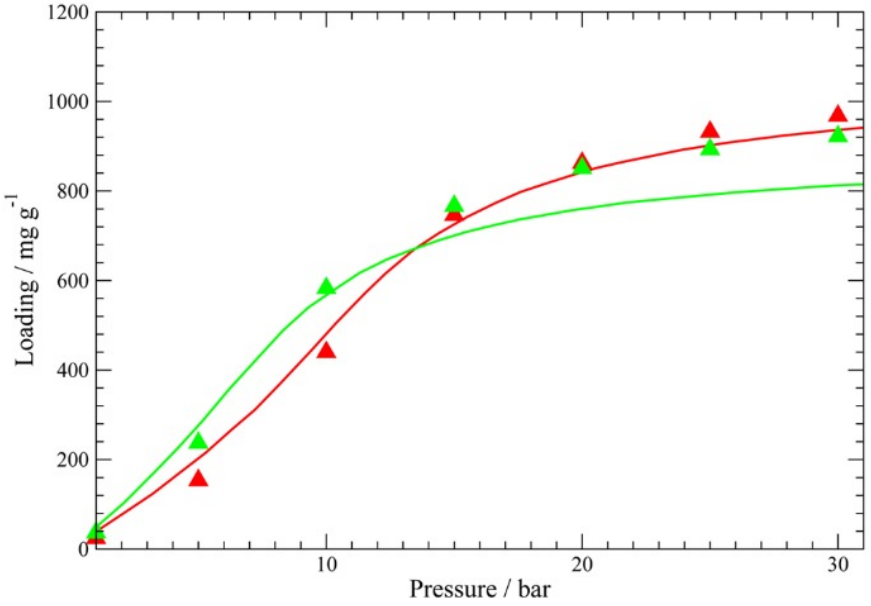

J. Phys. Chem. A ***2013****, 117, 10, 2053–2066*

Takeaways

- Take Home Message 1

Forcefield is set of empirical & physical

- Take Home Message 2

Include us, many people should keep focus more in “Physical meaning”

- Take Home Message 3

We have to respect the “Legacy”

Q&A